

Impact of new data for neutron-rich heavy nuclei on theoretical models for r -process nucleosynthesis

Toshitaka Kajino

Division of Theoretical Astronomy, NAOJ, 2-21-1 Osawa, Mitaka, Tokyo, 181-8588, Japan
Department of Astronomy, The University of Tokyo, 7-3-1 Hongo, Bunkyo-ku, Tokyo, 113-033, Japan
School of Physics and Nuclear Energy Engineering, Beihang University, Beijing 100191, China

Grant J. Mathews

Center for Astrophysics, University of Notre Dame, Notre Dame, IN 46556, USA
Division of Theoretical Astronomy, NAOJ, 2-21-1 Osawa, Mitaka, Tokyo, 181-8588, Japan

April 5, 2024

ABSTRACT

Current models for the r process are summarized with an emphasis on the key constraints from both nuclear physics measurements and astronomical observations. In particular, we analyze the importance of nuclear physics input such as beta-decay rates; nuclear masses; neutron-capture cross sections; beta-delayed neutron emission; probability of spontaneous fission, beta- and neutron-induced fission, fission fragment mass distributions; neutrino-induced reaction cross sections, etc. We highlight the effects on models for r -process nucleosynthesis of newly measured β -decay half-lives, masses, and spectroscopy of neutron-rich nuclei near the r -process path. We overview r -process nucleosynthesis in the neutrino driven wind above the proto-neutron star in core collapse supernovae along with the possibility of magneto-hydrodynamic jets from rotating supernova explosion models. We also consider the possibility of neutron star mergers as an r -process environment. A key outcome of newly measured nuclear properties far from stability is the degree of shell quenching for neutron rich isotopes near the closed neutron shells. This leads to important constraints on the sites for r -process nucleosynthesis in which freezeout occurs on a rapid timescale.

1. Introduction

Rapid neutron-capture (r -process) nucleosynthesis is responsible for the origin of approximately half of the elements heavier than iron and is the only means to produce the naturally occurring radioactive heavy actinide elements such as Th and U. However, in spite of more than a half century of study and observational progress [e.g. Sneden, Cowan & Gallino (2008)], the astrophysical sites for r -process nucleosynthesis have not yet been unambiguously identified (for reviews see, e.g., Arnould et al. (2007); Martínez-Pinedo (2008); Thielemann et al. (2011)). Although

many candidate sites have been proposed (Mathews & Cowan 1990), at present only neutron star mergers (NSMs) or core collapse supernovae (CCSNe) appear to be well suited as an r -process site. Nevertheless, there is still no consensus as to the correct astrophysical site. Indeed, it is undoubtedly the case that more than one astrophysical site has contributed to the observed Solar-System r -process abundances (Wehmeyer, Pignatari & Thielemann 2015; Shibagaki et al. 2016).

At least part of the reason for the difficulty in identifying the r -process site has been the lack of experimental data for the relevant neutron rich nuclei. However, in recent years the first systematic

direct measurements of properties of the very neutron rich nuclei relevant to r -process nucleosynthesis have become available. In this review we identify in part the impact that new measurements are having on the search for the site for the r -process.

Notwithstanding the difficulties in finding a suitable astronomical environment, the physical conditions for the r -process are well constrained (Burbidge et al. 1957) by simple nuclear physics considerations as described in following sections. It is evident that the r -process occurs via a sequence of near equilibrium rapid neutron captures and photo-neutron emission reactions far on the neutron-rich side of stability. This equilibrium is established with a maximum abundance strongly peaked on one or two isotopes far from stability. The relative abundance of r -process elements is then determined by the relative β -decay rates along this r -process path., i.e. slower β -decay lifetimes result in higher abundances. At least part of the reason for the difficulty in finding the astrophysical site for the r -process stems from the fact that it lies so far from the region of stable isotopes where until recently there has been little experimental data on nuclear masses, structure, and β -decay rates.

In this context, it is of particular interest that recently many masses and β -decay half-lives have been measured. For example, up to 110 neutron-rich isotopes of the elements from Rb to Sn have measured (Lorusso et al. 2015) at the RIKEN Radioactive Isotope Beam Factory. These isotopes encompass the neutron closed shell at $N = 82$. The new half-lives show evidence for new systematic features and exhibit a persistence of shell effects. The new data have helped to calibrate both beta-decay rates and new mass tables [e.g. (Nishimura et al. 2012; Möller et al. 2012; Lorusso et al. 2015)]. These measurements have direct implications for r -process calculations and reinforce the notion that the second ($A \approx 130$) and the rare-earth-element ($A \approx 165$) abundance peaks may result from the freeze-out of an $(n, \gamma) \rightleftharpoons (\gamma, n)$ equilibrium. In such an equilibrium, the new half-lives are important factors determining the relative abundance of rare-earth elements, and allow for a more reliable discussion of the r process environment.

Many of these newly measured isotopes are near or directly on the r -process path. As such,

they are of particular interest as they determine the β -flow toward the important r -process peak at $A = 130, N = 82$. Thus, they regulate the ability of models for the r -process to form heavier elements (Otsuki, Mathews & Kajino 2003; Shibagaki et al. 2016). It is of particular interest, therefore, to examine the impact of these new rates on the specific numerical models for r -process that we are most involved with. For further insight the reader is referred to many other recent reviews and sensitivity studies [e.g. Brett et al. (2012); Surman et al. (2014); Mumpower et al. (2016)] in the context of more schematic hot, cold, exponential time-dependence, adiabatic expansion, etc. r -process models.

We begin in Section 2 with a brief summary of key constraints from astronomical observations. In Section 3 we review the basic physics of the r process and highlight the required input nuclear data. Then, in Section 4 we summarize the input data available. In Section 5 we overview the main models for the r -process. In Section 6 we summarize the key directions the field has taken as a result of the present new data, and also describe some implications for understanding the galactic chemical evolution of the r process in Section 7. In Section 8 we summarize our (admittedly biased) view of what new data may be most desired in future measurements. We conclude in Sections 9 with a summary of the status of r -process models based upon the current data.

2. Observational Constraints

The present understanding of the origin of r -process elements has been helped greatly by the detailed elemental abundance distributions observed in r -process enhanced metal-poor stars in the Galactic halo (Snedden, Cowan & Gallino 2008). A key point is that the elemental abundances for these stars appear to identically match the Solar-System r -process abundances. This apparent “universality” in r -process abundances argues (Mathews & Cowan 1990; Argast et al. 2000, 2002, 2004) in favor of a single r -process environment that occurred early in the history of the Galaxy.

However, it is anticipated that universality may not extend to the elements Sn, Sb, I, and Cs, making the detection of these elements in metal-

poor stars of the utmost importance to determine the exact conditions of individual r -process events. Moreover, the scatter in the [Eu/Fe] abundances at low metallicity argues that the r -process is a rare event (Mathews & Cowan 1990; Mathews, Bazan & Cowan 1992; Ishimaru & Wanajo 1999; Argast et al. 2002, 2004). Indeed, the two most popular models for the r -process, NSMs or magneto-hydrodynamic jets (MHDJ), are indeed rare events compared to the event rate of normal core-collapse supernovae. More recently, it has been noted (Roederer et al. 2014) that stars that exhibit r -process enhanced abundances do not exhibit the same enhancement in α elements (although the α elements are indeed enhanced). This suggests that the α elements are not enhanced to the same degree as the r process when the r -process occurs in CCSN or NSMs. This supports the idea that the r -process is a rare event.

Recently, new insight has been gained from the observation of r -process elements in dwarf galaxies (Okamoto et al. 2008; Frebel et al. 2010, 2012; Ji et al. 2016; Roederer et al. 2016). For the most part, dwarf galaxies show r -process abundances similar to that of the Galactic halo (Frebel et al. 2012). However, the recent observations (Ji et al. 2016; Roederer et al. 2016) of seven stars in the dwarf galaxy Reticulum II, show evidence of a rare single event that ejected a large mass ($\sim 0.2 M_{\odot}$) of r -process elements. Such an event is strongly suggestive of a neutron star merger that is inherently a rare event and capable of ejecting a large mass of r -process elements. However, some magneto-hydrodynamically driven jet models may also produce a comparable mass.

In these metal-poor stars in the Reticulum II, enhanced α elements Mg and Ca are also detected. Very interestingly these are at the same level as Sr, Y, Zr and Ba, i.e. [X/Fe] \approx 0.5 to 1, except for extremely enhanced [Eu/Fe] \approx 1.5 to 2 (Roederer et al. 2016). It was previously noted (Roederer et al. 2014) that metal-poor stars in the Milky Way halo that exhibit r -process enhanced abundances do not necessarily exhibit the same enhancement in lighter elements. Although Na and Al are indeed not enhanced, the α elements like Mg, Si and Ca are enhanced. The existence of α elements in the metal-poor stars of Reticulum II and the Milky Way halo suggests that the α elements were ejected to the same degree as the

r process elements when the r -process occurred in the rare event like a NSM or MHDJ in the early Galaxy. Note, however, that it is difficult for NSMs to eject lighter elements with $A < 100$ as will be discussed in Section 6.

The lack of light elements in NSMs could also affect the dust formation (Takami et al. 2014). Dust grains have difficulty forming in the ejecta from NSMs due to the low number density of the lighter elements. Lighter elements like carbon and silicon, for example, are required for the condensation of silicon carbide X-grains that are classified to be supernova grains. Such grains may not be able to form in the ejecta of NSMs.

Another significant recent bit of observational evidence concerns the ‘kilonova’ light curve from short duration gamma-ray bursts (Tanvir et al. 2013; Berger, Fong & Chornock 2013). A faint ‘kilonova’ transient following the burst is attributed to the decay of neutron-rich radioactive species generated during the merger of two neutron stars. The near infrared emission also exhibits excess flux possibly due to the high opacity of the newly synthesized heavy elements. This provides evidence of active heavy-element nucleosynthesis in NSMs supporting this environment as a site for r -process nucleosynthesis.

3. Basics of the r -Process

The r process involves a sequence of rapid neutron captures in an explosive environment (Burbidge et al. 1957; Mathews & Ward 1985). Although many sites have been proposed for the r -process, whatever the environment, it can be shown that the Solar-System r -process abundances are well reproduced by beta-decay flow in a system that is in approximate $(n, \gamma) \rightleftharpoons (\gamma, n)$ equilibrium. Hence, the relative abundances of isotopes of a given element are determined by nuclear statistical equilibrium (NSE) as described by the nuclear Saha equation (Saha 1921).

$$\frac{n(Z, A)}{n(Z, A + 1)} = \frac{1}{n_n} \left(\frac{2\pi\mu kT}{h^2} \right)^{3/2} \times \frac{G_A G_n}{G_{A+1}} e^{-Q_n/kT}, \quad (1)$$

where μ is the reduced mass of the neutron plus isotope ${}^A Z$, h is Planck’s constant, k is the Boltzmann constant, and T is the temperature. The

quantity G_A is the partition function for nucleus, ${}^A Z$, Q_n is the neutron capture Q value for isotope ${}^A Z$ (or equivalently the neutron separation energy for the nucleus ${}^{A+1}Z$), and $n(Z, A)$ represents the number density of an isotope ${}^A Z$. Note, however, that this formula neglects a small correction (Mathews et al. 2011) for the difference between Maxwellian and Planckian distribution functions for the photons.

Equation (1) defines a sharp peak in abundances for one (or a few) isotopes within an isotopic chain. The flow of beta decays along these peak isotopes is then known as the r -process path.

The location of the r -process path peak is roughly identified (Burbidge et al. 1957) by the condition that neutron capture ceases to be efficient once $n(Z, A+1)/n(Z, A) \lesssim 1$. Taking the logarithm of Eq. (1) and inserting the numerical terms, the r -process path can be identified by the following relation

$$\left(\frac{Q_n}{kT}\right)_{\text{path}} = 2.30 \left(35.68 + \frac{3}{2} \log\left(\frac{kT}{\text{MeV}}\right) - \log\left(\frac{n_n}{\text{cm}^{-3}}\right) \right).$$

The elemental abundances $n(Z, A)$ along this path are then determined by the flow of beta decays,

$$\frac{dn(Z, A)}{dt} = \lambda_{Z-1} n(Z, A-1) - \lambda_Z n(Z, A), \quad (2)$$

where the total beta decay rate of each element along the path is given by the weighted sum of beta decay rates for each isotope $\lambda_\beta(Z, A) = 1/\tau_\beta(Z, A)$:

$$\lambda_Z = \sum_A n(Z, A) \lambda_\beta(Z, A) \quad (3)$$

For a typical r -process temperature of $T_9 \sim 1$, the requirement that the r -process path reproduce the observed abundance peaks at $A = 80, 130$ and 195 , implies that the r -process path halts at waiting points in the beta flow near the neutron closed-shell nuclei ${}^{80}\text{Zn}$, ${}^{130}\text{Cd}$ and ${}^{195}\text{Tm}$. For a neutron density sufficiently high ($n_n \gtrsim 10^{20} \text{ cm}^{-3}$) so that the neutron capture rates exceed the beta-decay rates for these isotopes, the peak abundances along the r -process path must be for isotopes with $Q_n \sim 1-3 \text{ MeV}$, and thus $(Q_n/kT)_{\text{path}} \sim 10-30$.

This constraint on Q_n , however, concerns the conditions near "freezeout" when the final neutrons are exhausted at the end of the r -process. At this point, the system falls out of NSE and nuclei along the r -process path decay back to the line of stable isotopes.

Earlier in the r process the neutron densities can be quite high and the r -process path shifted to more neutron-rich nuclei. For example, in the neutrino driven wind (NDW) models of Woosley et al. (1994), the r -process conditions begin with a neutron density of $n_n \approx 10^{27} \text{ cm}^{-3}$ and a temperature of $T_9 \sim 2$. The density is also much higher ($> 10^{32} \text{ cm}^{-3}$) when the material is first ejected from the proto-neutron star. Such conditions can also be achieved for an r process which occurs during NSMs (Freiburghaus, Rosswog & Thielemann 1999; Rosswog et al. 1999, 2000; Korobkin et al. 2012; Piran, Nakar & Rosswog 2013; Rosswog et al. 2013).

Of course, as the r process freezes out, one must make a detailed accounting of the full r -process reaction network, i.e.

$$\begin{aligned} \frac{dn(Z, A)}{dt} = & n(Z, A-1)\phi_n\sigma_{n,\gamma}(Z, A-1) \\ & + n(Z, A+1)\phi_\gamma\sigma_{\gamma,n}(Z, A+1) \\ & + n(Z-1, A)\lambda_\beta(Z-1, A) \\ & + \text{terms with } (n, p), (n, \alpha), (p, \gamma), (\alpha, \gamma), \\ & + (n, \text{fission}), (\beta, n), (\beta, \text{fission}), \text{ etc.} \\ & - n(Z, A)[\phi_n\sigma_{n,\gamma}(Z, A) + \lambda_\beta(Z, A) \\ & + \phi_\gamma\sigma_{\gamma,n}(Z, A) + \dots] \end{aligned} \quad (4)$$

where ϕ_n and ϕ_γ are the time-dependent neutron and photon fluxes, respectively. Recent work (Mumpower, McLaughlin & Surman 2012; Mumpower et al. 2015a; Mumpower et al. 2015b; Mumpower et al. 2016) has demonstrated that nuclear properties of a few isotopes in the range of $Z \approx 53-60, N \approx 100-115$ can have a dramatic effect on the final freezeout abundances for the rare-earth peak.

4. Nuclear Input Data

4.1. Nuclear Reaction Network

The nuclear reaction network is a key part of the nucleosynthesis simulations. An r -process network typically consists of more than 4000 isotopes,

including neutrons, protons, and heavy isotopes with atomic number $Z \leq 100$ [for example, see Table 1 in Nishimura et al. (2006)]. As noted above, nuclear reactions are most important as the system falls out of (n, γ) equilibrium where residual neutron captures can smooth the odd-even effect in the abundance distribution and shift the final abundances. They are also important in the build up of light nuclei to form the r -process seed nuclei (Sasaqui et al. 2005)

4.2. Nuclear Reaction Rates

The most important nuclear reaction rate for the r -process is the neutron capture rate for isotopes along the r -process path when the system falls out of (γ, n) equilibrium. In addition to neutron capture, one should also consider other possible reactions related to the r -process involving two- and three-body reactions or decay channels. Also, one should include electron capture as well as positron capture and screening effects for all of the relevant charged particle reactions.

4.3. New Measurements of Neutron Capture Rates

Available experimentally determined and theoretical neutron-capture reaction rates for r -process nucleosynthesis are maintained in REA-CLIB (Cyburt et al. 2010), and the Karlsruhe Database of Nucleosynthesis in Stars (KADoNiS) (Dillmann et al. 2006; Rauscher 2012). As theoretical estimates become better constrained by measurements near the r -process path, a better identification of the r -process site will follow.

Unfortunately, neutron capture rates along the r -process path are exceedingly difficult to measure. There is, however, the possibility (Reifarh & Litvinov 2014) that the combination of a radioactive beam facility, an ion storage ring and a high flux reactor would allow a direct measurement of inverse neutron capture reactions for isotopes with half lives down to \sim minutes. The idea is that radioactive ions pass through a neutron target. A storage ring of radioactive ions could be used to enhance the luminosity.

Even without direct measurements, however, useful information can be inferred (Chiba et al. 2008b; Jones et al. 2011; Kozub et al. 2012) using (d, p) reactions near the r -process path at

$A = 130, N = 82$. For example, in Kozub et al. (2012), direct-semi-direct (n, γ) cross section calculations were made, based for the first time on experimental data. The uncertainties in these cross sections were thus reduced by orders of magnitude compared to that of previous estimates.

Another possibility is to infer (γ, n) cross sections using virtual photons from Coulomb excitation with a radioactive ion beam. This technique has been successfully demonstrated in (Utsunomiya & Goriely 2012). In that paper a γ -ray strength function method was devised to determine radiative neutron capture cross sections for unstable nuclei along the valley of beta-stability. This method is based on the γ -ray strength function which interconnects radiative neutron capture and photoneutron emission within the statistical model. The method was applied to several unstable nuclei such as $^{93,95}\text{Zr}$, ^{107}Pd , and $^{121,123}\text{Sn}$. This method offers a versatile application extendable to unstable nuclei far from the stability when combined with Coulomb dissociation experiments at RIKEN-RIBF and GSI.

4.4. Theoretical Neutron Capture Rates

The nuclear reaction flow in the r process occurs in the vicinity of the neutron drip line. There are two main theoretical approaches for neutron capture reactions. These are: 1) via a compound nucleus (including resonances) as in the Hauser Feshbach estimates; 2) direct capture and semi-direct (DSD) processes. For most applications of r -process nucleosynthesis, nuclear cross sections have been based upon a simple estimate of the direct and semi-direct cross sections in terms of pre-equilibrium γ emission (Akkermans & Gruppelaar 1985), or in the context of Hauser-Feshbach theory, [e.g., Koning, Hilaire & Duijvestijn (2004); Young, Arthur & Chadwick (1992); Rauscher & Thielemann (2000); Cyburt et al. (2010)]. Such an approach can be justified when it is applied to nuclei in the vicinity of the stability line. However, in the neutron-rich region relevant to the r process, the neutron separation energies are diminished, so the compound nuclei may not have enough level density to compete with the compound elastic process. In this case, the compound capture cross section may be suppressed, and direct capture becomes dominant even at low energies.

Normally, the direct process is not very important because its cross section is much smaller than the compound capture cross sections. However, in Mathews et al. (1983) it was noted that far from stability where the level density is low, the direct capture process could be the dominant mode of neutron capture reaction for the r -process.

In Chiba et al. (2008a) the DSD components of the neutron capture cross sections were calculated for a number of tin isotopes by employing a single-particle potential (SPP) that gives a good reproduction of the known single-particle energies (SPEs) over a wide mass region. The results were compared with the Hauser-Feshbach contribution in the energy region of astrophysical interest. Their calculations showed that the Hauser-Feshbach component drops off rapidly for the isotope ^{132}Sn and toward more neutron-rich nuclei, whereas the DSD component decreases gradually and eventually becomes the dominant reaction mechanism. In (Chiba et al. 2008a) the reason for the difference in the isotopic dependence between the Hauser-Feshbach and DSD components was discussed, and its implication for r -process nucleosynthesis was given.

This result is consistent with those of previous studies, but the dependence of the DSD cross section on the target mass number is a feature of their SPP that gave a smooth variation of SPEs. As a consequence, the direct portion of the DSD components gave the largest contribution to the total (n, γ) cross section for neutron-rich isotopes below a few MeV. Therefore, the direct capture process modifies significantly the astrophysical (n, γ) reaction rates. The semi-direct component, however, gives a negligible contribution to the astrophysical reaction rates, but its impact is significant above several MeV.

Valuable studies of the impact of varying theoretical neutron capture rates in r -process models can be found in Mumpower et al. (2016). In those papers a Monte Carlo variation of Hauser-Feshbach neutron capture rates within the context of several mass models was explored. Crucial isotopes in the vicinity of the r -process peaks at $A = 130$ and 195 were identified and also in the vicinity of the rare-earth peak whose measurement would be most effective in reducing the uncertainties in r -process abundance calculations.

4.5. Nuclear Masses

Experimentally determined masses (Audi & Wapstra 1995; Audi, Wapstra & Thibault 2003; Wang et al. 2012) should be adopted if available. Otherwise, the theoretical predictions for nuclear masses are necessary. At present there are many available theoretical mass estimates far from stability. A good resource for nuclear masses can be found at <http://nuclearmasses.org>.

Theoretical mass tables for r -process nuclei are mainly based upon three approaches. One is the macroscopic/microscopic method based upon a liquid droplet formula plus shell corrections. The most popular adaptation of this is the finite range droplet model (FRDM) (Möller et al. 1995, 2012). Another variant of the macroscopic/microscopic approach is the phenomenological hybrid KTUY model (Koura et al. 2000, 2005). A third is the DZ model (Duffo & Zicker 1999) based upon a parametrization of multipole moments of the nuclear Hamiltonian. In a sense the DZ is more fundamental than the macroscopic/microscopic models. However, it is not strictly a microscopic theory, since no explicit nuclear interaction appears in the formulation.

At the next level would be masses based upon the extended Thomas Fermi random phase approximation (ETSFI) plus Strutinsky integral semi-classical approximation to a Hartree Fock (HF) approach (Aboussir et al. 1995; Pearson et al. 1996). The most microscopic extrapolations generally available of masses for neutron rich nuclei are those based upon the Skyrme Hartree-Fock Bogolyubov (HFB) method. This is a fully variational, approach with single-particle energies and pairing treated simultaneously and on the same footing. Some recent formulations include: HFB-19, HFB-21 (Goriely, Chamel & Pearson 2010); Gogny HFB (Goriely et al. 2009); the Skyrme-HFB (Goriely, Chamel & Pearson 2009; Chamel, Goriely & Pearson 2008); HFB-15 (Goriely & Pearson 2008); HFB-14 (Goriely, Samyn & Pearson 2007).

A good comparison of the relative merits of each approach can be found in Pearson & Goriely (2006). All approaches give a reasonable fit to known nuclear masses. However, there can be large deviations as one extends the mass tables to unknown neutron rich nuclei. Hence, there is a need for experimental mass determinations for

neutron rich nuclei.

A recent study has been made (Martin et al. 2016) of the impact of nuclear mass uncertainties based upon six Skyrme energy density functionals based on different optimization protocols. Uncertainty bands related to mass modeling for r -process abundances were determined for realistic astrophysical scenarios. This work highlights the critical role of experimental nuclear mass determinations for understanding the site for r -process nucleosynthesis.

4.6. New Experimental Masses

There are now active programs at CERN, GSI, RIKEN, JYFL, ANL, and NSCL to measure experimental masses on and near the r -process path. In particular, masses adjacent to the classical waiting-point nuclide ^{130}Cd have been measured (Atanasov et al. 2015) using the Penning-trap spectrometer ISOLTRAP at ISOLDE/CERN. That work reported a significant deviation (~ 400 keV) from earlier mass estimates based upon nuclear beta-decay endpoint data. The new measurements indicated a reduction of the $N = 82$ shell gap below the doubly magic nucleus ^{132}Sn .

A similar conclusion was reached in Hakala et al. (2012) based upon mass measurements at JYFL. This has a significant impact on models for the r process in either CCSNe or NSMs as reported in that paper.

4.7. Nuclear Structure Studies

The level structure of nuclei along the r -process path is important both as a means to determine the partition functions and as a means to test the strength of shell closures. Recently a number of studies have been completed (Watanabe et al. 2013; Simpson et al. 2014; Taprogge et al. 2014) in the neighborhood of the $N = 82, A = 130$ r -process peak. In particular, the first ever studies (Watanabe et al. 2013) of the level structure of the waiting-point nucleus ^{128}Pd and ^{126}Pd have been completed. That study indicated that the shell closure at the neutron number $N = 82$ is fairly robust. Hence, there is conflicting evidence between the nuclear masses and nuclear spectroscopy as to the degree of shell quenching near the $N = 82$ closed shell. It will be important to clarify this point as it has important implications for the site

of r -process nucleosynthesis as discussed below.

4.8. Beta-Decay Rates

The β -decay rates, particularly at waiting point nuclei, constitute one of the most important nuclear physics inputs to nucleosynthesis calculations in the r -process. Theoretical investigations of the beta decay of isotones with neutron magic number of $N = 82$ have been done by various methods including the shell model (Zhi et al. 2013), quasiparticle random-phase approximation (QRPA)/finite-range droplet model (FRDM) (Möller, Pfeiffer & Kratz 2003), QRPA/extended Thomas-Fermi plus Strutinsky integral (ETFSI) (Borzov & Goriely 2000)], and Hartree-Fock-Bogoliubov (HFB) + QRPA (Engel et al. 1999) calculations as well as in the continuum quasiparticle random-phase approximation (CQRPA) (Borzov 2003). The half-lives of nuclei obtained by these calculations are rather consistent with one another, and especially in shell-model calculations experimental half-lives at proton numbers $Z = 47, 48$, and 49 are well reproduced (Martínez-Pinedo & Langanke 1999).

For the β decays at $N = 126$ isotones, however, half-lives obtained by various calculations differ from one another (Langanke & Martínez-Pinedo 2003; Grawe, Langanke & Martínez-Pinedo 2007). First-forbidden (FF) transitions become important for these nuclei in addition to the Gamow-Teller (GT) transitions in contrast to the case of $N = 82$.

A strong suppression of the half-lives has been predicted in Borzov (2003) for $N = 126$ isotones due to the FF transitions. Most shell-model calculations of the β -decay rates of $N = 126$ isotones have been done with only the contributions from the GT transitions included (Langanke & Martínez-Pinedo 2003; Martínez-Pinedo et al. 2001). Moreover, as noted below experimental data for the β decays in this region of nuclei are not yet available. The region near the waiting point nuclei at $N = 126$ is therefore called the blank spot region.

In Suzuki et al. (2012), β decays of $N = 126$ isotones were studied by taking into account both the GT and FF transitions to evaluate their half-lives. Shell-model calculations were done with the use of shell-model interactions based upon modi-

fied G-matrix elements that reproduce well the observed energy levels of the isotones with a few (two to five) proton holes outside ^{208}Pb (Steer et al. 2008; Rydström et al. 1990).

In Marketin, Huther & Martínez-Pinedo (2015) the impact of first-forbidden transitions on decay rates was studied using a fully self-consistent covariant density functional theory (CDFT) framework to provide a table of β -decay half-lives and β -delayed neutron emission probabilities, including first-forbidden transitions. This work demonstrated that there is a significant contribution of the first-forbidden transitions to the total decay rate of nuclei far from the valley of stability. This also brings better agreement with experimentally determined half lives as discussed below.

In addition to ground state β decay, at the high temperatures of the r -process environment decay can proceed through thermally excited states. In Famiano et al. (2008) a calculation was made to evaluate the possible effects of the β -decay of nuclei in excited-states on the astrophysical r -process. Single-particle levels were calculated in the FRDM model with quantum numbers determined based upon their proximity to Nilsson model levels. The resulting rates were used in an r -process network calculation. Even though the decay rate model was simplistic, this work did provide a measure of the possible effects of excited-state β -decays on r -process freeze-out abundances. The main result of that work was that in the more massive nuclei, the speed up of the decay rates in the approach to closed shells tended to exaggerate the underproduction of nuclei below the nuclear closed shells as discussed below.

4.9. New Experimental Beta Decay Rates

There are currently many active programs to measure β -decay rates for nuclei near the r -process path (Dillmann et al. 2003; Pfeiffer et al. 2001; Hosmer et al. 2005; Montes et al. 2006; Hosmer et al. 2010; Quinn et al. 2012; Madurga et al. 2012; Benlliure et al. 2012; Benzoni et al. 2012; Domingo-Pardo et al. 2013; Kurtukian-Nieto et al. 2014; Morales et al. 2014; Lorusso et al. 2015). Even so, not all half-lives of nuclei most relevant to the r -process have been measured in the vicinity of either the $N = 50$ or $N = 82$ closed shells. Moreover, though experiments have provided valuable information for half-lives approaching the first and

second r -process peaks, so far no experimental half-lives are available for r -process nuclei at the important rare-earth peak or the third r -process peak at the $N = 126$ closed shell. However, next-generation facilities such as FRIB, ARIEL, RIBF, RISP SPIRAL2, ISOLDE upgrade, RIBLL, and FAIR will hopefully soon extend the list of measured isotopes to heavier nuclei on and near the r -process path.

4.10. Beta-Delayed Neutron Emission

Beta-delayed neutron emission is particularly important for the freezeout of the r -process. Recently, beta-delayed neutron emission probabilities of neutron rich Hg and Tl nuclei have been measured (Caballero-Folch et al. 2016) together with beta-decay half-lives for 20 isotopes of Au, Hg, Tl, Pb, and Bi in the region of neutron number $N \geq 126$. These are the heaviest nuclear species for which neutron emission has been observed.

Although not directly on the r -process path, these measurements have provided information with which to evaluate the viability of nuclear microscopic and phenomenological models for the high-energy part of the beta-decay strength distribution. Indeed, this study indicated that there is no global beta-decay model that provides satisfactory beta-decay half-lives and neutron branchings on both sides of the $N = 126$ shell closure. There was, however, a slight preference for the Hartree-Bogoliubov model of Marketin, Huther & Martínez-Pinedo (2015).

4.11. Fission Barriers and Fission Fragment Distribution

In r -process models with a very high neutron-to-seed ratio (such in the ejecta from neutron star mergers) the r -process path can proceed until neutron-induced or beta-induced fission terminates the beta flow at $A \sim 300$. Determining where this occurs can significantly impact the yields from r -process models (Eichler et al. 2015; Shibagaki et al. 2016). Unfortunately there are no measurements of fission barriers or fission fragment distributions (FFDs) for nuclei heavier than ^{258}Fm (Schmidt & Jurado 2012).

This is a major uncertainty in all calculations of fission recycling in the r -process. Shibagaki et al. (2016) considered a FFD model based upon the

KTUY model plus a two-center shell model to predict both symmetric and asymmetric FFDs with up to three components. As such, fissile nuclei could span a wide mass range ($A=100-180$) of fission fragments as demonstrated below.

On the other hand, the r -process models of Korobkin et al. (2012) were mostly based upon a simple two fragment distribution as in Panov, Freiburghaus & Thielemann (2001) (or alternatively the prescription of Kodama & Takahashi (1975)). The assumption of only two fission daughter nuclei tends to place a large yield near the second r -process peak leading to a distribution that looks rather more like the solar r -process abundances. In contrast, the FFDs of Goriely et al. (2013) are based upon a rather sophisticated SPY revision (Panebianco et al. 2012) of the Wilkinson fission model (Wilkins, Steinberg & Chasman 1976). The main ingredient of this model is that the individual potential of each fission fragment is obtained as a function of its axial deformation from tabulated values. Then a Fermi gas state density is used to determine the main fission distribution. This leads to a FFDs with up to four humps.

An even more important aspect is the termination of the r -process path and the number of fissioning nuclei that contribute to fission recycling and the freezeout of the r -process abundances. The r -process path in Shibagaki et al. (2016) proceeded rather below the fissile region until nuclei with $A \sim 320$, whereas the r -process path in (Goriely et al. 2013) terminates at $A \approx 278$ [or for a maximum $\langle Z \rangle$ for Korobkin et al. (2012)]. Moreover, Shibagaki et al. (2016) found that only $\sim 10\%$ of the final yield comes from the termination of the r -process path at $N = 212$ and $Z = 111$, while almost 90% of the $A = 160$ came from the fission of more than 200 different parent nuclei mostly via beta-delayed fission. On the other hand, the yields of Goriely et al. (2013) that are almost entirely due to a few $A \approx 278$ fissioning nuclei with a characteristic four hump FFD. As noted below, this has a dramatic impact on the final r -process abundance distribution.

5. Current Models for the r -Process

In spite of its simplicity, as noted above, the unambiguous identification of the sites for r -process

nucleosynthesis has remained elusive. The required high neutron densities and short explosive time-scales (\sim seconds) suggest that both CCSNe and NSMs are viable candidates for r -process nucleosynthesis. Observations (Snedden, Cowan & Gallino 2008) showing the appearance of heavy-element r -process abundances early in the history of the Galaxy seem to favor the short stellar lifetime of CCSNe as the r -process site. However, identifying the r -process site in models of CCSNe has been difficult (Arnould et al. 2007; Thielemann et al. 2011).

5.1. Neutrino Driven Wind Model

For a number of years, a favored model for r -process nucleosynthesis was in the neutrino driven wind (NDW) above the newly forming neutron star in CCSNe (Woosley et al. 1994). In this model, as a neutron star is formed by the collapse of the iron core of a massive star, the cooling of the proto-neutron star is characterized by the release of $\sim 10^{53}$ ergs in neutrinos on a timescale of ~ 10 sec. The interaction of these neutrinos with material behind the outgoing supernova shock generates a hot bubble that helps to drive the explosion (Bethe & Wilson 1995). It also leads to the ablation of material from the proto-neutron star into the hot bubble. This has been dubbed a neutrino-driven wind.

Although the original formulation was quite successful, in subsequent calculations the NDW has been shown (Fischer et al. 2010; Hüdepohl et al. 2010) to be inadequate as an r -process site when modern neutrino transport methods are employed along with a stiff nuclear equation of state (Warren 2016) as required by observations (Demorest et al. 2010; Antoniadis et al. 2013) of neutron stars with masses as large as $2.01 \pm 0.04 M_{\odot}$.

Of particular importance in this regards. It has been shown (Olson et al. 2016) that by adopting a Skyrme density functional equation of state that is consistent with constraints on the symmetry energy from the combination of isobaric analog states, pygmy resonances, and heavy ion collisions, that the decrease in neutrino energies and luminosity results. Hence, the likelihood of a NDW r -process has been affected by measurements that constrain the nuclear EoS and in particular, the density dependence of the nuclear symmetry energy. The result is that the desired conditions

of high entropy and neutron-rich composition (Otsuki et al. 2000; Otsuki, Mathews & Kajino 2003) do not occur in the neutrino energized wind. Nevertheless, it is quite likely that the so-called "weak r -process" occurs in the NDW producing neutron rich nuclei up to about $A \sim 125$ (Wanajo 2013; Shibagaki et al. 2016).

5.2. Neutron Star Mergers

Indeed, the difficulties in reproducing the r -process abundances have motivated many new studies of NSMs either as $NS + NS$ or $NS + BH$ binaries [e.g. Goriely et al. (2011); Korobkin et al. (2012); Piran, Nakar & Rosswog (2013); Rosswog et al. (2013, 2014); Goriely et al. (2013); Wanajo, et al. (2014); Nishimura et al. (2016)].

The ejected matter from NSMs is very neutron-rich ($\langle Z/A \rangle \equiv Y_e \sim 0.1$). This means that the r -process path can proceed along the neutron drip line all the way to the region of fissile nuclei ($A \approx 300$). Indeed, in such models, fission recycling occurs. That is, after the r -process terminates by beta-induced or neutron-induced fission, the fission fragments continue to experience neutron captures until fission again terminates the r -process path thereby repeating the process. After a few cycles the abundances become dominated by the fission fragment distributions and not as much by the beta-decay flow near the closed shells. Hence, nuclear data to constrain theoretical models of nuclear fission modes and mass distributions become very important.

Recent studies (Goriely et al. 2011; Korobkin et al. 2012; Goriely et al. 2013; Wanajo, et al. 2014; Nishimura et al. 2016) have indicated that the r process in NSMs produces a final abundance pattern that can be similar to the solar r -process abundances, but only for heavier $A > 130$ nuclei. However, it is possible (Shibagaki et al. 2016) that the main effects of fission recycling may be to fill in the bypassed abundances in the main r -process as discussed below.

However, the distribution of nuclear fission products can affect the final abundance pattern significantly. One must carefully extrapolate fission fragment distributions (FFDs) to the vicinity of the r -process path [cf. Martínez-Pinedo et al. (2007); Erler et al. (2012)]. It can be argued (Shibagaki et al. 2016), however, that by incor-

porating the expected broad distribution of fission fragments, the effect of the neutron closed shells becomes smoothed out, thereby providing a means to fill in the isotopes bypassed in the main r process.

The study of Shibagaki et al. (2016) made use of self consistent β -decay rates, β -delayed neutron emission probabilities, and β -delayed fission probabilities taken from Chiba et al. (2008a) and based upon fits to known fragment distributions. The spontaneous fission rates and the α -decay rates were taken from Koura (2004). For these rates β -delayed fission is the dominant nuclear fission mode near the termination of the r process (Chiba et al. 2008a). However, this is a phenomenological model. Current microscopic calculations tend to produce lower fission barriers and narrower fragment distributions as discussed below.

5.3. Magneto-hydrodynamic Jet Models

Although the NDW model does not seem to be a good source for the main r process, one scenario for r -process nucleosynthesis in CCSNe remains viable. It is the magneto-hydrodynamic jet (MHDJ) supernova model (Nishimura et al. 2006; Winteler et al. 2012; Nishimura, Takiwaki & Thielemann 2015). In this model magnetic turbulence leads the ejection of neutron rich material into a jet. As the jet transports this neutron-rich material away from the star it can undergo r -process nucleosynthesis in a way that avoids the problems associated with neutrino interactions in the NDW model. Moreover, the required conditions of the r -process environment (timescale, neutron density, temperature, entropy, electron fraction, etc.) are well accommodated in this model. Such jet models also have the advantage that they can naturally provide a site for a strong but rare r -process early in the early history of the Galaxy as required from astronomical observations.

The main features of the MHDJ supernova model are described in detail in Nishimura et al. (2006) and Winteler et al. (2012). We briefly outline the content of each model here. In Nishimura et al. (2006) two-dimensional MHD simulations were carried out from the onset of the core collapse to the shock propagation to the silicon-rich layers (~ 500 ms after bounce). Thereafter, the r -process nucleosynthesis was calculated

in the later phase by employing the two kinds of time extrapolations of the temperature and density starting from the composition produced the explosion.

A jet-like explosion could be formed from the combined effects of rapid rotation (ratio of rotational energy to gravitational energy $T/W \approx 0.5\%$) and a strong initial magnetic field ($\sim 10^{13}$ G). This jet had a lower electron fraction than in spherical explosions. As the ejected material with low Y_e in the jet emerged from the silicon layers, an r process occurred that was able to reproduce the solar r -process abundance distribution up to the third ($A \approx 195$) peak.

Winteler et al. (2012) expanded upon earlier MHDJ simulations by utilizing a three-dimensional magneto-hydrodynamic core-collapse supernova model and also including an approximate treatment of the neutrino transport. As in the two-dimensional calculations, in order to form the bipolar jets, a rare progenitor configuration characterized by a high rotation rate ($T/W \approx 0.8\%$) and a large magnetic field (5×10^{12} G) was required. This magnetic field was amplified to $\sim 10^{15}$ G during collapse by the conservation of magnetic flux. As in Nishimura et al. (2006) the low Y_e material ejected in the jet underwent r -process nucleosynthesis that reproduced the second and third peaks of the solar r -process element distribution.

However, all of these jet simulations tend to underproduce nuclides just below and above the r -process abundance peaks. This tendency is affected by the new measurements of masses and β -decay rates near the closed neutron shells along the r -process path as discussed below.

5.4. Collapsar r Process

There has been some interest (Fujimoto et al. 2006, 2007, 2008; Surman et al. 2008; Ono et al. 2012; Nakamura et al. 2013, 2015) in the possibility of r -process nucleosynthesis in the relativistic jets associated with the collapsar (failed supernova) model for gamma-ray bursts. See Nakamura et al. (2013, 2015) for a recent review. Collapsars are a favored model for the formation of observed long-duration gamma-ray bursts (GRBs). In the collapsar model (Woosley 1993; Paczynski 1998; MacFadyen & Woosley 1999; MacFadyen,

2001; Popham, Woosley & Fryer 1999; Aloy et al. 2000; Zhang, Woosley & MacFadyen 2003) the central core of a massive star collapses to a black hole. Angular momentum in the progenitor star, however, leads to the formation of a heated accretion disk around the nascent black hole. Magnetic field amplification and heating from the pair annihilation of thermally generated neutrinos emanating from this accretion disk can then launch material in a polar funnel region leading to an outflow of neutron-rich matter from the accretion disk into a relativistic jet along the polar axis.

A large volume of work has explored the formation of such collapsars [e.g. Takiwaki et al. (2004); Kotake, Yamata & Sato (2003); Sawai, Kotake & Yamada (2005); Obergaulinger et al. (2006); Suwa et al. (2007); Burrows et al. (2007); Takiwaki, Kotake & Sato (2009); Taylor, Miller & Podsiadlowski (2011), See also references in Kotake, Sato & Takahashi (2006)], and the development of the associated relativistic jets [e.g. MacFadyen & Woosley (1999); MacFadyen, Woosley & Heger (2001); Popham, Woosley & Fryer (1999); Aloy et al. (2000); Zhang, Woosley & MacFadyen (2003); Proga & Begelman (2003); Hawley & Krolik (2006); Minu, Hardee & Nishikawa (2007); Fujimoto et al. (2006); McKinney & Narayan (2007); Komissarov & McKinney (2007); Nagataki et al. (2007); Barkov, & Komissarov (2008); Nagakura et al. (2011)].

The work of Nakamura et al. (2015) utilized a model from Harikae et al. (2009) for slowly rotating collapsar models in axisymmetric special relativistic magneto-hydrodynamics (MHD). A method (Harikae et al. 2010) was also applied to compute the detailed neutrino-pair heating by ray-tracing neutrino transport to explore whether the collapsar model is indeed capable of generating the high entropy per baryon and neutron-rich material required for an r -process in a high-Lorentz-factor jet heated via neutrino-pair annihilation. Hydrodynamic studies of material in the heated jet along with the associated nucleosynthesis were evolved out to the much later times and lower temperatures associated with the r process.

It was found (Nakamura et al. 2015) that this environment could indeed produce an r -process-like abundance distribution. However, the very rapid time scale and high entropy caused the abundances to differ from the solar abundance distribution as shown in Figure 1. This is an extreme example of a model with a very rapid freezeout. As

noted below, new information on nuclear masses and β -decay rates near the r -process path now place important constraints on such models.

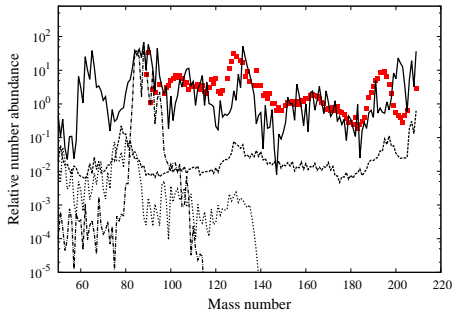


Fig. 1.— Summed mass-weighted abundance distribution (solid line) for the 1289 ejected tracer particles ejected in the collapsar jet [from Nakamura et al. (2015)]. These are compared with the Solar-System r -process abundances (points) (Käppeler, Beer & Wisshak 1989) and normalized at ^{153}Eu . Also shown are arbitrarily normalized abundances of elements synthesized in individual trajectories with high entropy $S/k = 1000$ (dashed), intermediate entropy $S/k = 100$ (dotted), and low entropy $S/k = 25$ (dash-dotted).

5.5. The tr -Process

It has been pointed out (Boyd et al. 2012) that the abundance patterns observed for the stars that do not fit the standard r -process template might be produced by stars that are sufficiently massive that their core collapse at first produces neutron stars. Subsequently, however, the infall onto the proto-neutron star causes a collapse to a black hole. This is the so-called fallback supernova. Stars in this class span a mass range from roughly 25 to 40 solar masses (Heger et al. 2002) for low-metallicity stars. When the neutron star collapses to a black hole the ongoing r -process ceases, terminating either when the r -processed regions are swallowed by the black hole or when the electron antineutrinos fall below the event horizon (Sasaqui, Kajino & Balantekin 2005). Thus, this truncated r -process, or tr -process, nucleosynthesis could terminate at different stages what would have been a normal neutrino-driven wind r -process, depending on the precise time at which

the black hole prevented further r -process production or emission of nuclides into the interstellar medium. In this paradigm, therefore, the delayed collapse to the black hole, combined with the difficulties in observing the higher mass rare-earth elements, could suggest a cutoff in the r -process distributions observed around $A \approx 165$. The implementation of this scenario then simply assumes that mass layers that produce the lighter r -process nuclei are ejected prior to those that produce the heavier r -process nuclides as in NDW models (Woosley et al. 1994). However, any setting within a core-collapse supernova that satisfies this condition could lead to a truncated r -process.

For this process as in the models noted above the nucleosynthesis is sensitive to the nuclear masses, beta decay rates, and neutron separation energies, but in this case the relevant atomic mass numbers are for light nuclei, $A < 100$. As a possible additional benefit of the tr -process, it was noted in Boyd et al. (2012) that in some cases the stars produced no nuclides in the $A = 130$ peak or beyond. This could have the effect of enhancing the yields of the lightest r -process nuclides relative to the main r process. Hence, this could provide an alternative means to fill in nuclei in the $A = 110 - 120$ region. Indeed, evidence in metal poor stars of the production of nuclides in the $A = 110 - 120$ mass region and lighter may indicate a tr -process origin. This conclusion, however, is very dependent upon nuclear properties of the light neutron-rich nuclei along the r -process path and requires a much more detailed simulation of the relevant astrophysics.

6. Impact of New Data on Models for the r Process

6.1. Impact on the MHD Jet model

There is a persistent problem in the MHDJ model, or any model [e.g. Otsuki, Mathews & Kajino (2003)] in which the r -process elements are produced on a short time scale via the rapid expansion of material away from the neutron star. Most such models underproduce isotopic abundances just below and above the r -process abundance peaks. Figure 2 from Shibagaki et al. (2016) illustrates why this occurs.

This figure shows an example of a typical calculated r -process path near the $N = 82$ neutron

closed shell just before freezeout when the neutrons are exhausted and the synthesized nuclides begin to beta decay back to the region of stable isotopes. Neutron captures and photo-neutron emission proceed in equilibrium for nuclei with a neutron binding energy of about 1-2 MeV. For r -process models with a rapid transport time, the density diminishes rapidly so that a sudden freezeout occurs close to the r -process path. However, above and below a closed neutron shell the r -process path shifts abruptly toward the closed shell from below (or away from the closed shell for higher nuclear masses). This shifting of the r -process path causes isotopes with $N = 70 - 80$ ($A \sim 110-120$) or $N = 90-100$ ($A \sim 140-150$) to be bypassed in the beta-decay flow. Indeed, this was a consistent feature in the original realistic NDW models of Woosley et al. (1994). This effect was apparent in many r -process calculation since the 1970s [cf. review in Mathews & Ward (1985)].

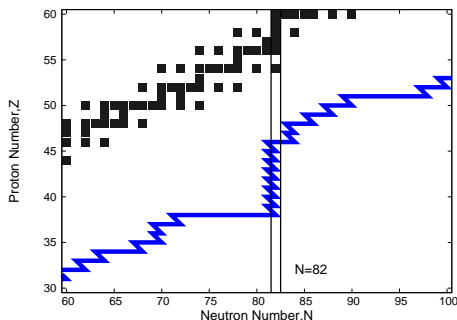


Fig. 2.— Illustration (Shibagaki et al. 2016) of the (N, Z) path of r -process nucleosynthesis (blue line) for nuclei with $A \sim 90 - 150$ in the vicinity of the $N = 82$ neutron closed shell just before freezeout of the abundances. Black squares show the stable isotopes.

Although it has been speculated for some time [e.g. Woosley et al. (1994); Pfeiffer et al. (2001); Farouqi et al. (2010)] that this could be due to quenching of the strength of the shell closure or beta-decay rates near the closed neutron shell, this explanation seems unlikely. Recent measurements (Nishimura et al. 2011; Lorusso et al. 2015) of beta-decay half lives near the r -process path have confirmed (Nishimura et al. 2012) that the reason for this discrepancy cannot be attributed to uncertainties in nuclear beta-decay properties

of nuclei along the r -process path.

In Nishimura et al. (2012) the r -process abundances were calculated in an MHD jet-like explosion based upon the two-dimensional magnetohydrodynamic simulation of Nishimura et al. (2006). This study explored the impact of new beta-decay rates on models with rapid transport. The ejecta were evolved with 23 tracer particles to describe the evolution of the thermodynamic state variables. These were then post-processed to obtain the nucleosynthesis yields.

The r -process calculations (Nishimura et al. 2012) were based upon three different nuclear reaction networks. One of the networks utilized only the FRDM theoretical rates (Möller et al. 1995) from the REACLIB compilation (Rauscher & Thielemann 2000). The other two (RIBF and RIBF+) utilize the new experimental β -decay half-lives of 38 neutron-rich isotopes from Kr to Tc and two versions of the theoretical FRDM β -decay rates for the other isotopes. The RIBF network replaced the FRDM rates with the new measured rates where possible. The third network (RIBF+) was based on the RIBF network and FRDM rates with modified Q -values for (n, γ) and reverse reactions given by:

$$Q_+ = \begin{cases} Q - 0.3 \text{ [MeV]} & (97 \leq A \leq 103) \\ Q + 0.5 \text{ [MeV]} & (104 \leq A \leq 107) \\ Q + 1.0 \text{ [MeV]} & (108 \leq A \leq 115) \end{cases} \quad (5)$$

where Q is the theoretical Q -value (in MeV) obtained from the FRDM (Möller et al. 1995). These modified Q -values were adopted because they led to a better fit to the measured β -decay lifetimes away from stability.

In particular, the underproduction of isotopes near $A = 120$ became slightly less pronounced relative to predictions based upon the FRDM rates when the new measured rates were employed.

Figure 3 from Nishimura et al. (2012) shows the final integrated abundance distributions from all of the trajectories. These are compared to the Solar-System r -process abundance distribution of Arlandini et al. (1999). Here the effect of new rates becomes apparent. Although it was hoped that the newly measured β -decay rates in this mass region might shift the β -flow equilibrium thereby filling in the low abundances near $A \sim 120$. Figure 3 shows that the abundances

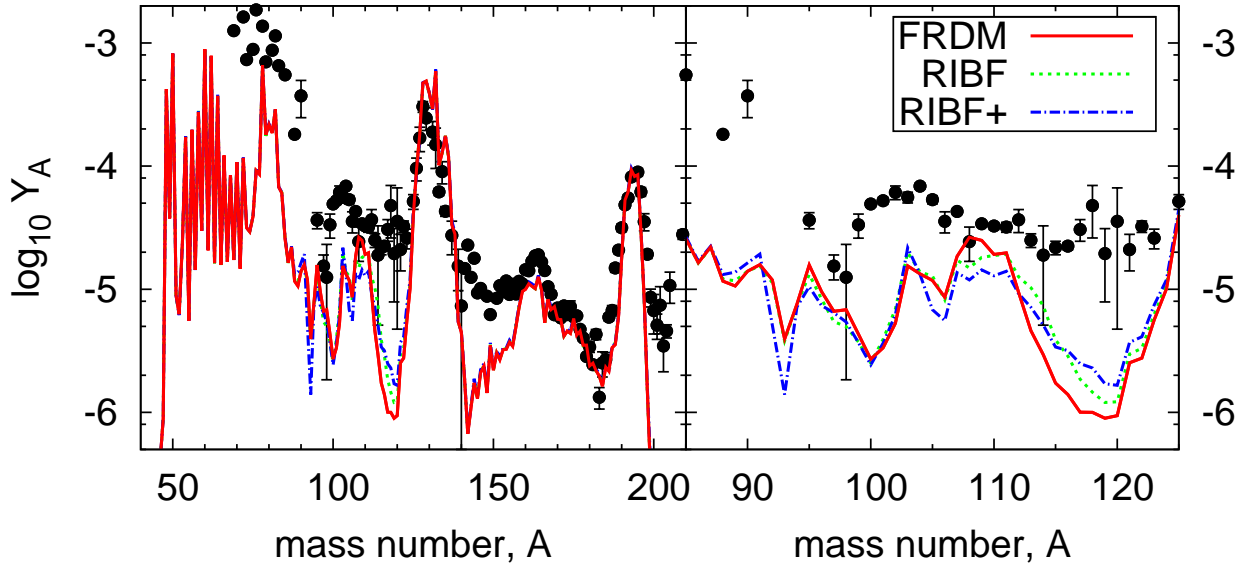


Fig. 3.— Integrated mass averaged total final abundance distributions of r -process elements from Nishimura et al. (2012) based upon the MHDJ supernova model (Nishimura et al. 2006). Red solid, green dotted, and blue dashed lines correspond to results from using the FRDM (standard), RIBF, and RIBF+ rates, respectively. Abundances of Solar-System r -process isotopes (Arlandini et al. 1999) are represented by black dots with error bars.

in the $A = 110 - 120$ region are only slightly enhanced. Thus, although the new rates provide a little assistance in enhancing the abundances below the abundance peak, they did not alleviate this problem. This suggested that a further modification of the r -process paradigm is required.

For example, Lorusso et al. (2015) were able to avoid the underproduction in a schematic high-entropy slower outflow model that summed over several wind trajectories similar to the NDW model. This effect is illustrated in Figure 4. A comparison between the upper plot without the new rates and the lower plot with the new rates indicates that the new rates have helped to fill in the discrepancies in abundances below and above the $A = 130$ r -process peak. However, this calculation was based upon a slow wind, not a rapid jet model. Since the wind models are now unviable as a means to produce the heaviest r -process nuclei, this does not solve the underproduction problem.

Similarly, Kratz et al. (2014) performed r -process calculations in a parameterized (slower

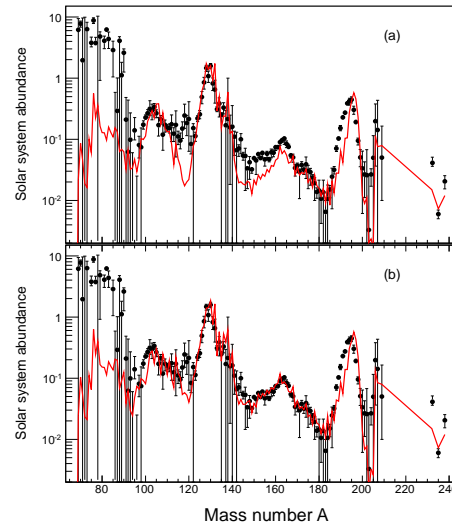


Fig. 4.— Comparison between schematic high-entropy wind model calculations (Lorusso et al. 2015) without the new beta decay rates (upper plot) and a calculation with the new rates (lower plot).

transport) NDW scenario based upon the models of Freiburghaus et al. (1999). Making use of new nuclear masses and beta-decay rates from the finite-range droplet model FRDM-(2012) (Möller et al. 2012) it was shown that the previous discrepancies near $A = 120$ are significantly diminished compared to the same calculation based upon the previous FRDM-(1992) (Möller et al. 1995) nuclear properties. Hence, one must keep in mind that at least some of the apparent discrepancy may be due to the adopted nuclear input. Indeed, this is a place where new measurements of nuclear masses near the r -process path have made an impact. In this case, the impact of the new beta-decay rates is to favor models with a more gradual freezeout near the end of the r process.

As another example, calculations of Nishimura et al. (2006) could fill the dips in an MHDJ model by using the ETFSI mass model. However, these models did so at the cost of displacing the 2nd and 3rd peaks and/or underproducing (or overproducing) abundances over a wide mass region between the second and third peaks.

6.2. Impact on Models for the r Process in Neutron Star Mergers

In Shibagaki et al. (2016) it was suggested that a solution to the underproduction of nuclei above and below the r -process abundance peaks can be obtained if one considers that both CCSNe and NSMs have contributed to the Solar-System r -process abundance distribution. Indeed, this solution not only resolves the dilemma of underproduction near the peaks, but may help to quantify the relative contributions of CCSNe vs. NSMs to the Solar-System r -process abundance distribution. However, this conclusion is very sensitive to the model for fission yields and beta-induced fission as described below.

In Shibagaki et al. (2016) r -process simulations were carried out in the NSM model based upon the merger outflow models of Korobkin et al. (2012); Piran, Nakar & Rosswog (2013); Rosswog et al. (2013). These were compared with abundances in the ejecta from the MHD supernova jet model of Nishimura et al. (2012) as well as weak r -process yields from the NDW models of Wanajo (2013). The NSM nucleosynthesis calculations were evolved using an updated version of the nuclear network code of Terasawa, Sumiyoshi, Kajino, Matheson & Tadin Winteler et al. (2012) to be "perhaps

(2001) with nuclear masses from the KTUY model (Koura et al. 2005) that have been shown (Nishimura et al. 2011; Lorusso et al. 2015) to reasonably well reproduce recently measured beta-decay half-lives of neutron-rich nuclei and also measured fission fragment distributions (Ohta, et al. 2007).

The red line on Figure 5 from Shibagaki et al. (2016) shows the result of their NSM nucleosynthesis simulation summed over all trajectories of material ejected from the binary NSM simulation. This is compared with the abundances in the ejecta from the MHD jet r -process (blue line) from Nishimura et al. (2012), and also the NDW weak r -process abundances (green line) produced in the neutrino driven wind from the 1.8 M_{\odot} supernova core calculation of Wanajo (2013).

The key point of this figure is the possible role that each process plays in producing the abundance pattern of Solar-System r -process abundances [black dots (Arlandini et al. 1999)]. The total abundance curve from all processes is shown as the black line on Figure 5. The abundances from each process were normalized by weighting factors f_{NSM} for NSMs and f_{Weak} for the NDW relative to the MHDJ yields that were normalized to the r -process abundance peaks. The best fit (black) line in Figure 5 is for $f_{NSM} = 0.3$ and $f_{Weak} = 5$.

These relative contributions are more or less consistent with Galactic event rates and expected mass ejection from the models. It was shown in Shibagaki et al. (2016) that weight parameters f_{NSM} and f_{Weak} can be deduced from observed Galactic event rates and expected yields, i.e.

$$f_{NSM} \approx \frac{R_{NSM} M_{r,NSM}}{\epsilon_{MHDJ} R_{CCSN} M_{r,MHDJ}}, \quad (6)$$

and

$$f_{Weak} \approx \frac{R_{CCSN} M_{r,Weak}}{\epsilon_{MHDJ} R_{CCSN} M_{r,MHDJ}}, \quad (7)$$

where $M_{r,NSM}$, $M_{r,MHDJ}$, and $M_{r,Weak}$ are the ejected mass of r -elements from the NSM, MHDJ, and NDW weak- r -process models, respectively, while R_{CCSN} and R_{NSM} are the corresponding Galactic event rates of CCSNe and NMSs. The quantity ϵ_{MHDJ} is the fraction of CCSNe that result in magneto-rotationally driven jets. This was

$\sim 1\%$ ” of the core-collapse supernova rate. However this is probably uncertain by at least a factor of two.

The mass of synthesized r -process elements from magneto-rotationally driven jets has been estimated (Winteler et al. 2012) to be $6 \times 10^{-3} M_{\odot}$ while that of a typical binary NSM is expected to be $(2 \pm 1) \times 10^{-2} M_{\odot}$ (Korobkin et al. 2012). If the Galactic NSM rate is $80_{-70}^{+200} \text{ Myr}^{-1}$ (Kalogera et al. 2004), and the Galactic supernova rate is, $(1.9 \pm 1.1) \times 10^4 \text{ Myr}^{-1}$ (Dhiel 2006), then it was estimated (Shibagaki et al. 2016) that $f_{NSM} \sim 0.6 \pm 0.4$ and $f_{Weak} \approx 8 \pm 6$ consistent with their fit parameters. Although the derivation in Shibagaki et al. (2016) is quite uncertain it at least supports the plausibility of this approach.

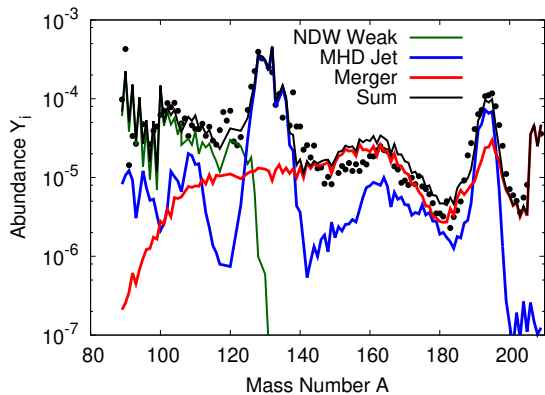


Fig. 5.— Average final abundance patterns [from Shibagaki et al. (2016)] for NSMs (red line), MHDJ (blue line) and the NDW weak r -process (green line) from Wanajo (2013). These are compared with the Solar-System (Arlandini et al. 1999) r -process abundances (black dots). The thin black line shows the sum of all contributions.

Of particular relevance is that the one order of magnitude underproduction of nuclides above and below the $A = 130$ r -process peak from the MHD jet model (shown by the blue line) is nearly accounted for by contributions from the NDW and NSM models.

The final r -process isotopic abundances from the NSM model of Shibagaki et al. (2016) exhibited a very flat pattern due to several episodes of fission cycling under extremely neutron-rich conditions. Thus, NSMs may resolve most of the underproduction problems of the MHDJ model pre-

dictions for the elements just below and above the abundance peaks and be largely responsible for the rare-earth abundances in the range $A = 140 - 180$. The remaining underproduction below the $A = 130$ peak could then be due to the NDW weak r -process as illustrated on Figure 5.

The conclusions of Shibagaki et al. (2016), however, were critically dependent upon the fission barriers and fragment distributions adopted in that study. An important difference between the work of Shibagaki et al. (2016) and that of other NSM studies (Goriely et al. 2011; Korobkin et al. 2012; Piran, Nakar & Rosswog 2013; Rosswog et al. 2013, 2014; Goriely et al. 2013; Wanajo, et al. 2014; Nishimura et al. 2016) is the termination of the r -process path.

The r -process path in the NSM calculations of Shibagaki et al. (2016) proceeds rather below the fissile region until nuclei with $A \sim 320$, whereas the r -process path based upon microscopic calculations of fission barriers [such as Goriely et al. (2013)] terminates at $A \approx 278$ [or for a maximum $\langle Z \rangle$ for (Korobkin et al. 2012)]. Also, in Shibagaki et al. (2016) only $\sim 10\%$ of the final yield came from the termination of the r -process path at $N = 212$ and $Z = 111$, while almost 90% of the $A \approx 160$ bump shown in Figure 5 was from the fission of more than 200 different parent nuclei mostly via beta-delayed fission. This is illustrated in the upper panel of Figure 6 from Shibagaki et al. (2016).

This is in contrast to the yields of Goriely et al. (2013) that are almost entirely due to a few $A \approx 278$ fissioning nuclei with a characteristic four hump FFD. It is important to keep in mind that many microscopic calculations of fission barriers are consistent with an early termination near $A \approx 280$. It is only the phenomenological fission probabilities (Koura 2004; Chiba et al. 2008a) that allow the r -process path to continue to $A > 300$. The difference in r -process abundances from the two possibilities is significant.

This point is illustrated in the lower panel of Figure 6. This figure compares with a calculation in which it was assumed that the r -process path was terminated by symmetric fission of nuclei with $A = 285$ [similar to that of Goriely et al. (2013)]. In this case a solar-like distribution is obtained similar to that of Goriely et al. (2011); Korobkin et al. (2012); Goriely et al. (2013). This

highlights the importance of eventual detailed measurements of fission barriers and fragment distributions for nuclei near the termination of the r -process path.

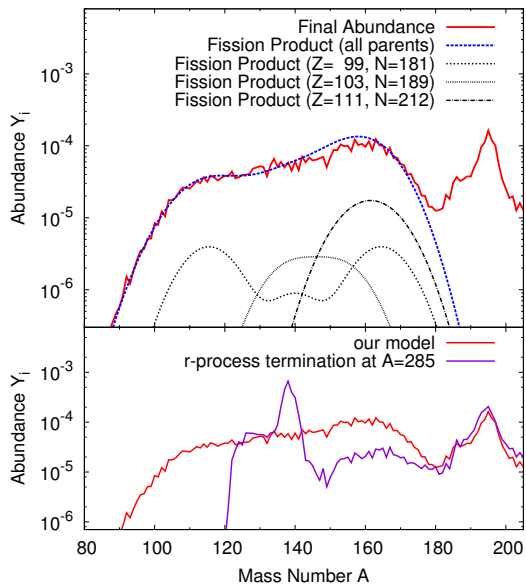


Fig. 6.— Illustration of the impact of fission yields and fission recycling on the final r -process abundances from Shibagaki et al. (2016). Upper panel shows the relative contributions for 3 representative nuclei compared with the final abundance distribution. The lower panel shows the same final r -process yields compared with the distribution that would result if the termination of the r -process path were to occur at $A = 285$.

7. Impact on Models for Galactic Chemical Evolution

In this review we suggest that the measured and best estimates of nuclear input masses and beta-decay rates near the r -process path support an r -process model in which the freezeout of abundances is slower than that of the MHD jet models. This may support a large contribution from NSMs. Although NSMs appear to make a good r -process site, chemical evolution studies (Mathews & Cowan 1990; Argast et al. 2000, 2002, 2004) have shown that very short merger times of NSMs are needed to reproduce abundances seen in r -enhanced extremely metal-poor

stars in the Galactic halo.

There are two possible scenarios for a large contribution from NSMs. One is that the first stars had a large contribution from MHDJ ejecta that was later supplanted by the contribution from NSMs. This possibility was considered in Shibagaki et al. (2016) where it was shown that the universality in *elemental* abundances for the low metallicity first stars is consistent with the MHD jet yields. This is because the isotopic sum to produced elemental abundances tends to fill in the missing isotopes above and below abundance peaks. However, some slight deviations from universality may appear in this scenario (Shibagaki et al. 2016). It would be valuable to look for evidence for such deviations in the most metal-poor r -enhanced stars.

Another possibility is that the time scale of metal enrichment in the most metal-poor stars does not follow a simple age-metallicity relation. That is, some of the enrichment of r elements may occur in dwarf galaxies that later merge with the Galactic halo.

Recently, Hirai et al. (2015) considered the chemical evolution in dwarf spheroidal galaxies (dSphs). Such dSphs are the building blocks of the Galactic halo and have a much lower star formation efficiency than that of the Milky way halo. That paper showed that when the effect of metal mixing was taken into account, the enrichment of r -process elements in dSphs by NSMs could reproduce the observed $[\text{Eu}/\text{Fe}]$ vs. metallicity distribution with a merger delay time of as much as 300 Myr. This is because metallicity is not really correlated with the time ~ 300 Myr from the start of the simulation to the low star formation efficiency in dSphs. They also confirmed that this model is consistent with observed properties of dSphs such as the radial profiles and metallicity distribution. A merger time of ~ 300 Myr and a Galactic NSM rate of $\sim 10^{-4} \text{ yr}^{-1}$ could reproduce the abundances of metal poor r -process enhanced stars and is consistent with the values suggested by population synthesis and other nucleosynthesis studies.

8. Summary of the most needed nuclear measurements

From the point of view of this review there are two main thrusts where new data would be most helpful. For understanding the MHDJ model, it is imperative to know the beta-decay rates above and below the r-process peaks at $A=130$ and 195 . Figure 7 (S. Nishimura, Priv. Comm.) summarizes the current situation of measurements at RIKEN until 2014 and what is accessible with a higher intensity uranium beam. This figure shows that a number of isotopes along the r-process path near the $N = 82$ closed neutron shell now have measured beta-decay lifetimes. However, a number of isotopes above the shell still need investigation. Moreover, for all of these nuclei precise nuclear masses must be determined, perhaps via beta-decay endpoint measurements. It is important to know the neutron separation energies to quantify the degree of shell quenching in this region. The reader is referred to Brett et al. (2012) for a list of the most important separation energies to measure near the $N = 82$ closed neutron shell and also Mumpower et al. (2016) for an exhaustive list of the most important isotopes and measurements in the context of various r -process paradigms. Also, nuclear spectroscopy needs to be completed for these isotopes to determine the nuclear partition functions.

In particular, beta decay lifetimes along the r -process path in the rare earth peak region and near the $A=195$ peak are crucial measurements. Even the simple question as to whether the r -process occurs in a cold or hot, or fission recycling environment could be answered if beta decay rates and masses are known near the rare-earth peak at $A \sim 160$ (Mumpower et al. 2016). In particular, nuclear properties of a few isotopes in the range of $Z \approx 53 - 60$, $N \approx 100 - 115$ can have a dramatic effect on the final freezeout abundances for the rare-earth peak (Mumpower et al. 2016). Eventually, beta-decay lifetimes and nuclear masses near the $A = 195$, $N = 126$ neutron closed shell are also desired as a means, in particular, to test the viability of the MHDJ model.

As also outlined in Mumpower et al. (2016) neutron capture rates along the r -process path are crucial for some isotopes near the $A = 130$ and $A = 195$ peaks and also near the rare-earth peak

at $A \sim 160$. As noted above, what is needed is an ambitious project for direct measurements using inverse kinematics and a storage ring, or indirect (d, p) and virtual (γ, n) measurements via Coulomb excitation of unstable beams.

Regarding neutron star mergers, it is critical to understand fission barriers, beta-induced fission rates and fission fragment mass distributions in the vicinity of the heaviest $A \sim 280 - 300$ nuclei near the termination of the r -process path. If fission barriers are low so that fission occurs via one or two isotopes near $A \sim 285$, and if this fission produces a bimodal distribution as microscopic calculations suggest (Goriely et al. 2013), then NSMs are a very viable candidate to produce the entire r -process abundances. On the other hand, if the r -process proceeds all the way to nuclei with $A \sim 300$ as in the study of Shibagaki et al. (2016), then NSMs may only contribute to the rare-earth peak plus help to fill the gaps above and below the r -process peaks. The best resolution of this question would be to directly measure fission barriers and beta-delayed fission in this region. This is a difficult measurement to make, but perhaps the formation of these nuclei in via a radioactive-ion reaction followed by beta decay into the region of fissile nuclei could be used to reveal the fission barriers and fission fragment mass distributions.

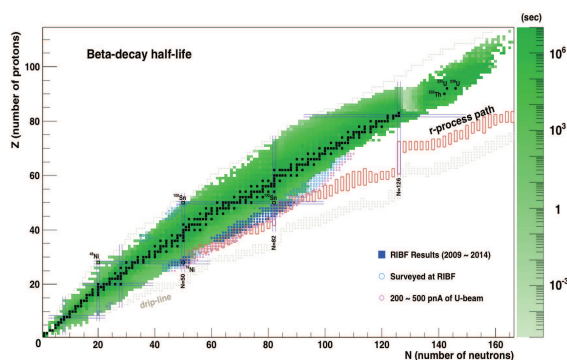


Fig. 7.— Illustration of the isotopes along the r -process path indicating those beta half lives that have been measured up to 2014 at RIKEN and those that may be accessible via a high intensity uranium beam in the future.

9. Conclusions

In this review we have considered the various models for r -process nucleosynthesis and how new measurements of β -decay rates and nuclear masses near the r -process path have impacted these models. A main impact of the new measurements concerns the tendency of models with a rapid freezeout timescale to underproduce isotopes below and above the main r -process abundance peaks.

Although the new mass data suggest some shell quenching around the neutron closed shells far from stability, the indication from the β -decay rates suggests that this quenching is not enough to prevent the underproduction in models with a rapid freezeout like MHD jets. Phenomenological models with a more gentle freezeout (as in the NDW) seem to best reproduce the r -process abundances. However, since NDW models are out of favor on theoretical grounds, the need for NSM contributions to the r process is apparent. Although material is tidally ejected at high velocity in NSMs, the freezeout can occur on a more gradual timescale in the frame of the ejected material due to the very high neutron density.

The question remains, however, as to whether the fission recycling environment of NSMs can reproduce all of a part of the r -process abundance distribution. The answer to that question will require the continual accumulation of masses, beta-decay rates, and in particular, fission barriers, and fission mass distributions for the heaviest neutron-rich nuclei near the termination of the r -process path.

This study was supported in part by Grants-in-Aid for Scientific Research of JSPS (19340074, 20244035, and 22540290), JSPS Fellows (21.6817), Scientific Research on Innovative Area of MEXT (20105004), and U.S. Department of Energy under Nuclear Theory Grant DE-FG02-95-ER40934. This work also benefited from support by the National Science Foundation under Grant No. PHY-1430152 (JINA Center for the Evolution of the Elements).

REFERENCES

Aboussir, Y. *et al.* 1995, *At. Data Nucl. Data Tables* 61 127

Aloy, M. A., Müller, E., Ibàñez, J. M., Martí, J. M., & MacFadyen, A. 2000, *ApJ*, 531, L119

Akkermans J. M. & Gruppelaar, H. 1985, *Phys. Lett.* B157, 95

Antoniadis, M. *et al.* 2013 *Sci*, 340, 448

Argast, D., Samland, M., Gerhard & O. E., Thielemann, F.-K. 2000, *A&A*, 356, 873

Argast, D., Samland, M., Thielemann, F.-K. & Gerhard, O. E. 2002, *A&A*, 388, 842

Argast, D., Samland, M., Thielemann, F.-K. & Y.-Z Qian 2004, *A&A*, 416, 997

Arlandini, C. *et al.* 1999, *ApJ*, **525**, 886

Arnould, M., Goriely, S. & Takahashi, K. 2007, *Phys. Rep.*, **450**, 97

Atanasov, D. *et al.* 2015, *Phys. Rev. Lett.* 115, 232501

Audi G. & Wapstra, A. H. 1995, *Nucl. Phys. A*, **595**, 409

Audi, G. Wapstra, A. H. & Thibault, C. 2003, *Nucl. Phys.* A729 337

Barkov, M. V. & Komissarov, S. S. 2008, *MNRAS*, 385, L28

Benlliure, J. *et al.* 2012, *J. Phys. Conf. Ser.*, 337, 012070

Berger, E., Fong, W. & Chornock, R. *ApJL*, 774, L23

Bethe, H. A. & Wilson, J. R. 1995, *ApJ*, 295,14

Benzoni, G. *et al.* 2012, *Phys. Lett. B* 715, 293

Borzov, I. N. & Goriely, S. 2000, *Phys. Rev. C* 62, 035501

Borzov, I. N. 2003, *Phys. Rev. C* 67, 025802

Boyd, R. N., Famiano, M. A., Meyer, B. S., Motizuki, Y., Kajino, T. & Roederer, I. U. 2012, *ApJL*, 744, L14

Brett, S., Bentley, I., Paul, N., Surman, R., Aprahamian, A. 2012, *EPJA*, 48, 184,

Burbidge, E. M. *et al.* 1957, *Rev. Mod. Phys.*, **29**, 547

- Burrows, A., Dessart, L., Livne, E., Ott, C. D. & Murphy, J. 2007, *ApJ*, 664, 416
- Caballero-Folch, R. et al. 2016, *Phys. Rev. Lett.*, 117, 012501
- Chamel, N., Goriely, S., Pearson, J.M. 2008, *Nuc. Phys. A*812, 72
- Chiba, S., Koura, H., Maruyama, T. *et al.* 2008, in *Origin of Matter and Evolution of Galaxies*, AIP Conf. Proc. 1016, 162
- Chiba, S., Koura, H., Hayakawa, T., Maruyama, T., Kawano, T. and Kajino, T., 2008, *Phys. Rev. C*77, 015809,
- Cybert, R. H. *et al.* 2010, *Astrophys. J. Suppl. Ser.* 189, 240
- Demorest, P. B. *et al.* 2010, *Nature*, 467, 1081
- Dhiel, R. *et al.* 2006, *Nature*, 439, 45
- Dillmann, I. *et al.* 2003, *Phys. Rev. Lett.* 91, 162503
- Dillmann, I., Heil, M., Kppeler, F., Plag, R., Rauscher, T. & Thielemann, F.-K. 2006, AIP Conf. Proc. 819, 123; online at <http://www.kadonis.org>
- Domingo-Pardo, C. *et al.* 2013, *Nuclear Physics in Astrophysics VI, Lisbon 2013*, Conf. Proc. arXiv:1309.3047 [nucl-ex].
- Duflo, J. & Zuker, A.P. 1999, *Phys. Rev. C*59 R2347.
- Engel, J., Bender, M., Dobaczewski, J., Nazarewicz, W. & Surman, R. 1999, *Phys. Rev. C* 60, 014302
- Eichler et al. 2015, *ApJ*, 808, 30
- Erler, J., Langanke, K., Loens, H. P., Martínez-Pinedo, G. & Reinhard, P.-G. 2012, *Phys. Rev. C*85, 025802
- Famiano, M. A. Boyd, R. N., Kajino, R. N., Otsuki, K., Terasawa, M. & Mathews, G. J. 2008, *J. Phys. G*, 35, 025203
- Farouqi, K., Kratz, K.-L.; & Pfeiffer, B. *et al.* 2010, *ApJ*, 712, 1359.
- Fischer, T. , Whitehouse, S. C., Mezzacappa, A. , Thielemann, F.-K. & Liebendörfer, F.-K. 2010, *Astron. Astrophys.* 517, 80
- Frebel, A. *et al.* 2010, *Nature*, 464, 72
- Frebel, A. & Volker, B. 2012, *Astrophys. J.* 759, 115
- Freiburghaus, C., Rembges, J.-F., Rauscher, T. *et al.* 1999, *ApJ*, 515, 381
- Freiburghaus, C., Rosswog, S. & Thielemann, F.-K. 1999, *ApJL*, 525, L121
- Fujimoto, S.-I., *et al.* 2006, *ApJ*, 644,1040
- Fujimoto, S.-I., *et al.* 2007, *ApJ*, 656, 382
- Fujimoto, S.-I., *et al.* 2008, *ApJ*, 680, 1350
- Goriely, S. Hilaire, S. & Koning, A.J. 2008, *A&A*, 487, 767
- Goriely, S., Bauswein, A. & Janka, H.-T. 2011 *Astrophys. J. Lett.* 738, L32
- Goriely S., *et al.* 2013, *Phys. Rev. Lett.*, 111, 242502
- Goriely, S. Chamel, N. & Pearson, J. M. 2010, *Phys. Rev. C* 82 035804
- Goriely, S. Hilaire, S., Girod, M. & Peru, S. 2009, *Phys. Rev. Lett.* 102 242501
- Goriely, S. Chamel, N. & Pearson, J. M. 2009, *Phys. Rev. Lett.* 102 152503
- Goriely, S. & Pearson, J.M. 2008, *Phys. Rev. C* 77 031301(R)
- Goriely, S. Samyn, M. & Pearson, J.M. 2007, *Phys. Rev. C* 75 064312
- Grawe, H., Langanke, K. & Martínez-Pinedo, G. 2007, *Rep. Prog. Phys.* 70, 1525
- Hakala, J. 2012, *Phys. Rev. Lett.* 109, 032501
- Harikae, S. *et al.* 2009, *ApJ*, 704, 354
- Harikae, S. *et al.* 2010, *ApJ*, 713, 304
- Hawley, J. F., & Krolik, J. H. 2006, *ApJ*, 641, 103
- Heger, A., Fryer, C. L., Woosley, S. E., Langer, N., & Hartmann, D. H. 1992, *ApJ*, 591, 288

- Hirai, Y., Ishimaru, Y., Saitoh, T. R., Fujii, M. S., Hidaka, J. & Kajino, T. 2015, *ApJ*, 814, 41
- Hosmer, P. T. *et al.* 2005, *Phys. Rev. Lett.* 94, 112501
- Hosmer, P. T. *et al.* 2010, *Phys. Rev. C* 82, 025806
- Hüdepohl, L., Müller, B., Janka, H.-T. Marek, A. & Raffelt, G. G. 2010, *Phys. Rev. Lett.* 104, 251101
- Ishimaru, Y. & Wanajo, S. 1999, *ApJL*, 511, L33
- Iwamoto, A., Yamaji, S., Suekane, S. & Harada, K. 1976, *Prog. Theor. Phys.* 55, 115
- Ji, A. P., Frebel, A., Chiti, A., & Simon, J. D. 2016, *Nature*, 531, 610
- Jones, K. L. *et al.* 2011, *Phys. Rev. C* 84, 034601
- Kalogera, V. *et al.* 2004, *Astrophys. J. Lett.* 614, L137 (2004).
- Käppeler, F., Beer, H., & Wisshak, K. 1989, *Rep. Prog. Phys.*, 52, 945
- Kodama, T., & Takahashi, K. 1975, *Nucl. Phys.* A239, 489
- Komissarov, S. S., & McKinney, J. C. 2007, *MNRAS*, 377, L49
- Koning, A. J., Hilaire, S. & Duijvestijn, M. 2004, *NRG Report 21297/ 04.62741/P FAI/AK/AK*, NRG, Petten, the Netherlands
- Korobkin, O., Rosswog, S., Arcones, A. & Winteler, C. 2012, *Mon. Not. Roy. Astro. Soc.* 426, 1940
- Kotake, K., Sato, K., & Takahashi, K. 2006, 69, 971
- Kotake, K., Yamada, S., & Sato, K. 2003, *ApJ*, 595, 304
- Koura, H., Uno, M., Tachibana, T. & Yamada, M. 2000, *Nucl. Phys. A* 674 47
- Koura, H. 2004, *Tours Symposium on Nuclear Physics V*, AIP Conf. Proc. 704, 60
- Koura, H., Tachibana, T., Uno, M. & Yamada, M. 2005, *Prog. Theor. Phys.* 113, 305
- Kozub, R. L. *et al.* 2012, *Phys. Rev. Lett.*, 109, 172501
- Kratz, K.-L., Farouqi, K. & Möller, P. 2014, *ApJ*, 792, 6
- Kurtukian-Nieto, T. 2014, *Eur. Phys. J. A* 50, 135 (2014).
- Langanke, K. & Martínez-Pinedo, G. 2003, *Rev. Mod. Phys.* 75, 818
- Lorusso, G. *et al.* 2015, *Phys. Rev. Lett.* 114, 19250
- MacFadyen, A. I. & Woosley, S. E. 1999, *ApJ*, 524, 262
- MacFadyen, A. I., Woosley, S. E., & Heger, A. 2001, *ApJ*, 550, 410
- Madurga, M. *et al.* 2012, *Physical Review Letters* 109, 112501
- Marketin, T. Huther, L & Martínez-Pinedo, G. 2015, *Phys. Rev. C* 93, 025805
- Martin, D., Arcones, A., Nazarewicz, W. & Olsen, A. 2016, *Phys. Rev. Lett.* 116, 121101
- Martínez-Pinedo, G. & K. Langanke 1999, *Phys. Rev. Lett.* 83, 4502
- Martínez-Pinedo, G. 2001, *Nucl. Phys. A* 688, 357
- Martínez-Pinedo, G. *et al.* 2007, *Prog. Part. Nucl. Phys.*, 59, 199
- Martínez-Pinedo, G. 2008, *J. Phys. G* 35, 014057
- Mathews, G. J., Bazan, G. & Cowan, J. J. 1992, *ApJ*, **391**, 719
- Mathews, G. J. & Ward, R. A. 1985, *Rep. Prog. Phys.*, 48, 1371
- Mathews, G. J., & Cowan, J. J. 1990, *Nature*, **345**, 491
- Mathews, G. J., Mengoni, A., Thielemann, F.-K. & and Fowler, W. A. 1983, *ApJ*, 270, 740
- Mathews, G. J., Pehlivan, Y., Kajino, T., Balantekin, A. B. and Kusakabe, M. 2011, *Astrophys. J.*, 727, 10
- McKinney, J. C., & Narayan, R. 2007, *MNRAS*, 375, 513

- Mizuno, Y., Hardee, P. & Nishikawa, K.-I. 2007, *ApJ*, 662, 835
- Möller, P. *et al.* 1995, *At. Data Nucl. Data Tables*, **59**, 185
- Möller, P., Nix, J. R. & Kratz, K.-L. 1997, *At. Data Nucl. Data Tables* 66, 131
- Möller, P., Pfeiffer, B. & Kratz, K.-L. 2003, *Physical Review C* 67, 055802
- Möller, P., Myers, W. D. Sagawa, H. *et al.* 2012, *PRL*, 108, 052501
- Montes, F. *et al.* 2006, *Phys. Rev. C* 73, 035801
- Morales, A.I. *et al.* 2014, *Phys. Rev. Lett.* 113, 022702
- Mumpower, M. R., McLaughlin, G. C. & Surman, R. 2012, *Phys. Rev. C* 86, 035803
- Mumpower, M. R. *et al.* 2015a, *Phys. Rev. C* 92, 035807
- Mumpower, M. R., Surman, R., Fang, D. L., Beard, M. & Aprahamian, A. 2015b, *J. Phys. G* 42, 034027
- Mumpower, M. R., Surman, R., McLaughlin G.C. & Aprahamian, A. 2016, *Prog. Part. Nucl. Phys.*, 86, 86
- Myers, W. D. & Swiatecki, W. J. 1999, *Phys. Rev. C* 60, 014606
- Nagakura, H. *et al.* 2011, *ApJ*, 731, 80
- Nagataki, S. *et al.* 2007, *ApJ*, 659, 512
- Nakamura, K. *et al.* 2013, *Int. J. Mod. Phys.*, E22, 133022
- Nakamura, K., Kajino, T., Mathews, G. J., Sato, S. & Harikae S. 2015, *A&A*, 582, A34 (2015).
- Nishimura, S. *et al.* 2011 *Phys. Rev. Lett.*, **106**, 052502
- Nishimura, S. *et al.* 2006, *ApJ*, **642**, 410
- Nishimura, S. *et al.* 2011, *Phys. Rev. Lett.*, 106, 052502
- Nishimura, N., Kajino, T. Mathews, G.J., Nishimura, S. & Suzuki, T. 2012, *Phys. Rev. C* 85, 048801
- Nishimura, N., Takiwaki, T. & Thielemann, F.-K. 2015, *ApJ*, 810, 109
- Nishimura, N. *et al.* 2016, *J. Phys. Conf. Ser.*, 665, 012059
- Ohta, M., *et al.* 2007, in *Proc. of Int. Conf. on Nucl. Data for Science and Technology*, Nice, France,
- Okamoto, S. Arimoto, N. Yamada, Y. & Onodera, M. 2008, *A&A*, 487, 103
- Olson, J. P. *et al.* 2016, *Phys. Rev. C*, Submitted
- Ono, M., Hashimoto, M., Fujimoto, S., Kotake, K. & Yamada, S. 2012, *Prog. Th. Phys.*, 128, 741
- Otsuki, K., Tagashi, H., Kajino, T., & Wanajo, S. 2000, *Astrophys. J.*, 544, 424
- Paczynski, B. 1998, *ApJ*, 494, L45
- Panebianco, S. *et al.* 2012, *Phys. Rev. C* 86 064601
- Panov, I. V., Freiburghaus, C. & Thielemann, F.-K. 2001, *Nuc. Phys. A* 688, 587
- Pearson, J.M. *et al.* 1996, *Phys. Lett. B* 387 455
- Pearson, J.M. Goriely, S. 2006 *Nuc. Phys. A* 777, 623
- Pfeiffer, B. *et al.* 2001, *Nucl. Phys. A* 693, 282
- Proga, D., & Begelman, M. C. 2003, *ApJ*, 592, 767
- Popham, R., Woosley, S. E., & Fryer, C. 1999, *ApJ*, 518, 356
- Obergaulinger, M., Aloy, M. A., Dimmelmeier, H., & Müller, E. 2006, *A&A*, 457, 209
- Otsuki, K., Mathews, G. J. & Kajino, T. 2003, *New Astronomy*, **8**, 767
- Piran, T., Nakar, E. & Rosswog, S. 2013, *Month. Not. Roy. Astro. Soc.* 430, 2121
- Quinn, M. *et al.* 2012, *Phys. Rev. C* 85, 035807
- Rauscher, T. & Thielemann, F.-K. 2000, *At. Data Nucl. Data Tables* **75**, 1
- Rauscher, T. 2012, *ApJL*, 755, L10
- Reifarh, R., Litvinov, Y.A. 2014, *Phys. Rev. Spec. Top. Acc. Beams* 17 014701.

- Roederer, I. U. *et al.* 2014, *Mon. Not. Roy. Astron. Soc.*, 445, 2970
- Roederer, I. U. *et al.* 2016, *Astron. J.*, 151, 82
- Rosswog, S., Liebendorfer, M., Thielemann, F.-K., *et al.* 1999, *A&A*, 341, 499
- Rosswog, S., Davies, M. B., Thielemann, F.-K., & Piran, T. 2000, *A&A*, 360, 171
- Rosswog, S. and Liebendorfer, M. 2003, *MNRAS*, 342, 673
- Rosswog, S. 2009, *New Astron. Rev.*, 53, 78
- Rosswog, S., Piran, T. & Nakar, E. 2013, *Mon. Not. Roy. Astro. Soc.* 430, 2585
- Rosswog, S., Korobkin, O., Arcones, A., Thielemann, F.-K. & Piran, T. 2014, *Mon. Not. Roy. Astron. Soc.*, 439, 744
- Rydström, L., Blomqvist, J., Liotta, R. J. & Pomar, C. 1990, *Nucl. Phys.* A512, 217
- Saha, M. N., 1921, *Proc. Roy. Soc. London, Ser. A*, 99, Issue 697 135
- Sasaqui, T., Kajino, T., & Balantekin, A. B. 2005, *ApJ*, 634, 534
- Sasaqui, T., Kajino, T., Mathews, G. J., Otsuki, K. & Nakamura, K. 2005, *ApJ*, 634, 1173
- Sato, K., Yamaji, S., Harada, K. & Yoshida, S. 1979, *Z. Phys. A* 290, 149
- Sawai, H., Kotake, K., & Yamada, S. 2005, *ApJ*, 631, 446
- Shen, H. Tok, K. Oyamatsu, K. Sumiyoshi, *Nucl. Phys. A*, 637, 435 (1998).
- Shen, H. Tok, K. Oyamatsu, K. Sumiyoshi, *Progress Theor. Phys.*, 100, 1013 (1998).
- Shibagaki, S., Kajino, T., Mathews, G. J., Chiba, S. Nishimura, S. and Lorusso, G. 2016, *ApJ*, 816, 79
- Simpson, G., *et al.* 2014, *Phys. Rev. Lett.* 113, 132502
- Schmidt, K.-H. and Jurado, B. 2012 *Phys. Proc.*, 31, 147
- Snedden, C. Cowan, J. J. & Gallino, R. 2008, *Ann. Rev. Astron. Astrophys.*, **46**, 241
- Steer, S. J. *et al.* 2008, *Phys. Rev.* C78, 061302
- Surman, R. *et al.* 2008, *J. Phys.* G35, 014059
- Surman, R.; Mumpower, M.; Cass, J.; Bentley, I.; Aprahamian, A.; McLaughlin, G. C. 2014, *EPJWC*, 66, 07024
- Suzuki, T., Yoshida, T., Kajino, T. & Otsuka, T. 2012, *Phys. Rev.* C85, 015802
- Suwa, Y., Takiwaki, T., Kotake, K. & Sato, K. 2007, *PASJ*, 59, 771
- Takami, H., Nozawa, T. & Ioka, K. 2014, *ApJL*, 789 L6
- Takiwaki, T., Kotake, K., Nagataki, S. & Sato, K. 2004, *ApJ*, 616, 1086
- Takiwaki, T., Kotake, K., & Sato, K. 2009, *ApJ*, 691, 1360
- Tanvir, N. R. *et al.* 2013, *Nature*, 500, 547
- Taprogge, J. *et al.* 2014, *Phys. Lett. B* 738 223.
- Tatsuda, S., Yamamoto, K., Asano, T. *et al.* 2008, in *Origin of Matter and Evolution of Galaxies*, AIP Conf. Proc. 1016, 469
- Taylor, P. A., Miller, J. C. & Podsiadlowski, Ph. 2011, *MNRAS*, 410,2385
- Terasawa, M., Sumiyoshi, K. Kajino, T., Mathews, G. J. & Tanihata, I. 2001, *Astrophys. J.* 562, 470
- Thielemann, F.-K. *et al.*, *Prog. Part. Nucl. Phys.*, **66**, 346 (2011).
- Travaglio, C. *et al.* 2004, *ApJ*, **601**, 864
- Utsunomiya, H. and Goriely, S. 2012 in *ORIGIN OF MATTER AND EVOLUTION OF GALAXIES 2011*, AIP Conf. Proc., 1484, pp. 150-155
- Valentim, R., Rangel, E. & Horvath, J. E. 2011, *Mon. Not. Roy. Astron. Soc.*, 414, 1427
- Wanajo, S. 2013, *Astrophys. J. Lett*, 770, L22
- Wanajo, S., Sekiguchi, Y., Nishimura, N. *et al.* 2014, *ApJL*, 789 L39

- Wang, M. *et al.* 2012, *Chin. Phys.*, C36 1603
- Warren, M. 2016, PhD Thesis, University of Notre Dame
- Watanabe, H. *et al.* 2013, *PRL*, 111 152501
- Wehmeyer B, Pignatari M, Thielemann FK 2015, *MNRAS* 452 1970
- Wilkins, B. D., Steinberg, E. P. & Chasman, R. R. 1976, *Phys. Rev. C*14, 1832
- Winteler, C., Käppeli, R., Perego, A. *et al.* 2012, *ApJL*, 750, L22
- Woosley, S. E. 1993, *ApJ*, 405, 273
- Woosley, S. E. & Heger, A. 2006, *ApJ*, 537, 810
- Woosley, S. E., & Heger, A. 2006, *Astrophys. J.*, 637, 914
- Woosley, S. E., Wilson, J. R., Mathews, G. J., Hoffman, R. D. & Meyer, B. S. 1994, *ApJ*, 433, 229
- Young, P. G. Arthur, E. D. & Chadwick, M.B. 1992, LA-12343-MS, Los Alamos National Laboratory
- Zhang, W., Woosley, S. E. & MacFadyen, A. I. 2003, *ApJ*, 586, 356
- Zhi, Q., Caurier, E., Cuenca-García, J. J., Langanke, K., Martínez-Pinedo, G. Sieja, K. 2013, *Physical Review C* 87, 025803